# Dispersion-Enhanced Volume Hologram for Dense Wavelength-Division Demultiplexer

Jie Qiao, Feng Zhao, Jian Liu, and Ray T. Chen, *Senior Member, IEEE*

***Abstract*—A fully packaged dense wavelength-division demultiplexer (DWDDM) by using dispersion-enhanced volume holographic grating and silicon V-grooved fiber array is demonstrated. The device demultiplexs eight optical channels within $C$ band with 2 nm wavelength spacing. The system insertion losses are $-5.68$, $-5.6$, $-5.40$, $-5.3$ , $-5.68$, $-5.59$, $-5.58$, and $-5.49$ dB, respectively. Typical cross-talks among these eight channels are less than $-35$ dB. The trade-off between getting smaller physical packaging size and linear dispersion ability at different wavelength is addressed. The device is designed for optical communications for Metropolitan area networks where both free space DWDM and multimode fiber band networks are jointly employed.**

***Index Terms*—Optical interconnects, photopolymer films, volume holographic grating, wavelength division demultiplexing.**

## I. Introduction

DENSE wavelength-division-multiplexing (DWDM) systems are key elements for increasing the transmission bandwidth of optical communications and sensors. The employment of DWDM systems allows the already installed point-to-point networks to greatly multiply their capacity without additional optical fibers. An important future of dense WDM is that discrete wavelengths from an orthogonal set of carriers which can be separated, routed, and switched without interfering with one another[1]–[3].

In this letter, an eight channel fully packaged dense wavelength division demultiplexer (DWDDM) is presented which employs a novel dispersion-enhanced grating design [9], using a path-reversed substrate-guided-wave configuration working at a center wavelength of 1555 nm. The polymer-based holographic grating lowers the cost of the device compared to using gratings made out of other materials. Multimode fibers enables the demultiplexer to resist the mechanical and environmental disturbance well. The lights are zigzagged within a wedge angled substrate which decreases the device size effectively. This demultiplexer is compact in size, reliable in operation, and more cost-effective compared with the counterparts made out of the other methods [4]–[8].

Manuscript received October 18, 1999; revised April 7, 2000. This work was supported by Ballistic Missile Defense Organization, Army SMDC, the Center of Optoelectronics Science and Technology (COST), DARPA, Office of Naval Research, AFOSR, Cray Research, DuPont, Lightpath, 3M Foundation, and the Advanced Technology Program (ATP) of the state of Texas.

The authors are with Microelectronics Research Center, Department of Electrical and Computer Engineering, University of Texas, Austin, TX 78758 USA (e-mail: jqiao@ece.utexas.edu).

Publisher Item Identifier S 1041-1135(00)06278-9.

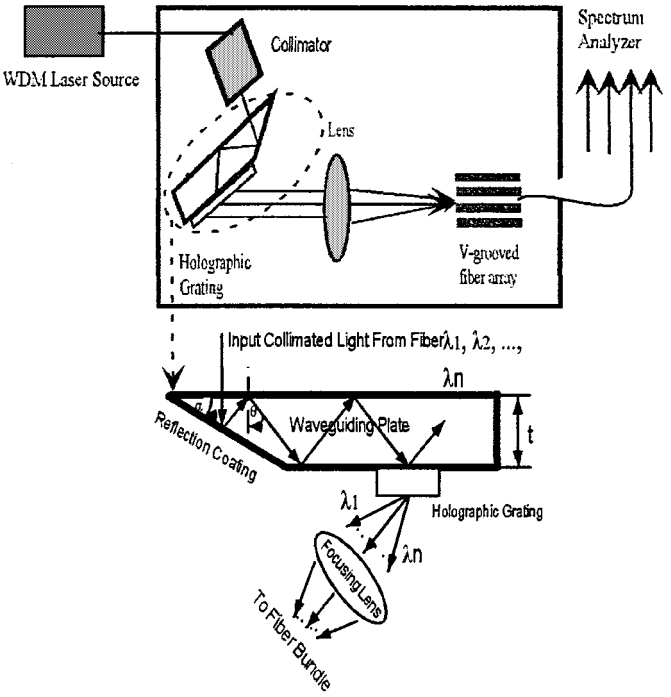


Fig. 1. (a) Schematic of eight channel DWDDM device and (b) geometric structure of a path-reversed substrated-guided-wave device.

## II. Grating Working Principle and Structure

A path-reversed photopolymer-based substrate-guided holographic grating is used for demutiplexing eight wavelengths with 2 nm separation. The choice of wavelengths and wavelength channel spacing is due to the requirement of the parallel optical interconnect system built by Jet Propulsion Lab [10]. Fig. 1 shows the schematic of the eight channel DWDDM device. The grating dispersion ability for the first order forward diffraction can be derived from grating equation [11], which gives

$$\frac{d\theta_{\text{diff}}}{d\lambda} = \frac{\sin\varphi}{\Lambda\cos\theta_{\text{diff}}} = \frac{n(\sin\theta_2' + \sin\theta_2)}{\lambda\cos\theta_{\text{diff}}} \tag{1}$$

where

- $\varphi$ slanted angle of grating;
- $\Lambda$ grating period;
- $\theta_2, \theta_2'$ incident angle and diffraction angle of the optical signals in the grating region at a center wavelength of $\lambda$ (in the air);
- $n$ average refractive index of the grating region;
- $\theta_{\text{diff}}$ designed diffraction angle in the air.

One can easily find that the larger the diffraction angle, the greater the angular dispersion. The larger the angular dispersion,

TABLE I
SPACING DEVIATION FOR TWO DIFFERENT GRATING STRUCTURE

| Wavelength (nm) | | 1549 | 1551 | 1553 | 1555 | 1557 | 1559 | 1561 | 1563 |
|---|---|---|---|---|---|---|---|---|---|
| Expected spacing to center wavelength | | -750 | -500 | -250 | 0 | 250 | 500 | 750 | 1000 |
| Deviations of spacing(um) | 60°/60° structure | -24.08 | -13.91 | -5.85 | 0 | -3.57 | -4.76 | -3.48 | 0.37 |
| | 60°/0° structure | -3.94 | -2.63 | -1.32 | 0 | -1.32 | -2.63 | -3.94 | -5.25 |

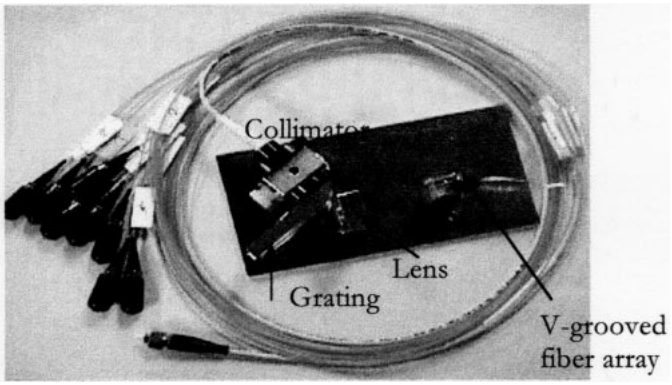


Fig. 2. Inside setup of the fully packaged eight-channeled DWDDM device.

the smaller the packaging size. Consequently large angular dispersion is always preferable in DWDM design.

The diffracted multiwavelength signals are coupled into a silicon V-grooved fiber array with a 62.5 $\mu$m diameter core, and a 250 $\mu$m channel spacing. The linearity of the angular dispersion among different wavelengths is pivotal to get balanced coupling efficiency. Since the grating angular dispersion is not an exact linear function, there is a small deviation from the designed diffraction position to the real diffraction position. Therefore, it is much easier to get high and balanced coupling efficiency if we could choose our wavelengths in the linear region of the dispersion equation. The condition for getting linear angular dispersions among different channels can be found by taking the second order derivative of $\theta_{\text{diff}}$, i.e.

$$\frac{d^2\theta_{\text{diff}}}{d\lambda^2} = \frac{\sin(\theta_{\text{diff}})}{\cos^3\theta_{\text{diff}}\Lambda_y^2}. \tag{2}$$

In equation (2), $\Lambda y = \Lambda/\sin(\varphi)$, it is the grating period projected in the direction vertical to the grating normal. When diffraction angle in the air is zero, The best angular dispersion linearity can be achieved. Diffraction angle at different wavelength is

$$\theta_{diff(\lambda)} = \arcsin(\lambda/\Lambda_y - n \times \sin(\theta_2)). \tag{3}$$

Channel spacing between the specific wavelength and the center wavelength is thus determined to be

$$\Lambda d_{(\lambda)} = f \times \tan(\theta_{\text{diff}(\lambda)} - \theta_{\text{diff(center}-\lambda)}). \tag{4}$$

In (4), $f$ is the focal length of the lens used for focusing the light spot down to diffraction limit. The simulation result of channel spacing deviation at two different incident angles and diffraction angles is shown on Table I. For incident angle of 60° in the air, diffraction angle of 0° in the air, (i.e., 60°/0° structure), we can get coupling balance, but the dispersion ability is 0.0485 degree per nanometer. For grating structure with incident angle of 60° in the air, diffraction angle of 60° in the air, (i.e., 60°/60° structure), the dispersion ability is 0.1600° per nm, which is 2.3 times bigger than that of 60°/0° structure. But the linearity of its angular dispersion is worse than that of 60°/0° structure. It means there exists a tradeoff between the dispersion ability and the dispersion linearity. For the 60°/60° structure, Most of the spacing deviation are smaller than 6 $\mu$m. Compared to the diameter of multimode fiber and the small light spot size which is close to diffraction limit, it is tolerable. The biggest one is 24.08 $\mu$m, which can be compensated by tuning wavelength slightly at the specific channel. We select a grating structure with a grating period $\Lambda$ of 694 nm, a diffraction angle $\theta_{\text{diff}}$ of 60° in air and an incident angle $\theta$ of 60° in the grating. This structure can provide a relatively large dispersion and bandwidth [11], $d\theta_{\text{diff}}/d\lambda = 0.16°$/nm. The beveled edge provides a way to overcome the limitation of the critical angle of the waveguiding substrate and to enhance the dispersion of the holographic grating (see Fig. 2).

## III. EXPERIMENT

As shown in Fig. 1, the lights coming from WDM lasers are transposed to a collimator by a polarization maintaining single mode fiber, and are diffracted by a 60°/60° holographic grating. Diffracted beams outside of grating vary almost linearly with the deviation of eight input wavelengths. A lens is used to focus the beams down to diffraction limited spots which can be coupled into an eight channel silicon V-grooved multimode fiber array. The device is designed for optical communications for Metropolitan area networks where both free space DWDM and multimode fiber band networks are jointly employed [12].

To maintain precision and accuracy during the packaging, the V-grooved fiber array is installed on a specially designed gripper whose position can be controlled by a position system with six degrees of freedom. First of all, We couple the center wavelength 1555 nm to the 4th channel of v-grooved fiber array which is the designed coupling channel for center wavelength. The smallest insertion loss and balanced crosstalk to the two neighboring channels can be reached by adjusting $X, Y, Z$ translation stage. At this time, the focus point of the lens is immediately on the front face of V-grooved fiber array when operating at the center wavelength. Similarly, the other seven wavelengths are coupled to correspondent channels with the smallest insertion loss and balanced crosstalks. The measured insertion losses and crosstalks of the DWDDM system are listed in Table II. The typical value of crosstalks is less than $-35$ dB which

TABLE II
INSERTION LOSSES AND CROSSTALKS OF THE PACKAGED DEVICE

| Channel # &Wavelength (nm) | 1 | 2 | 3 | 4 | 5 | 6 | 7 | 8 |
|---|---|---|---|---|---|---|---|---|
| 1. ( 1549.45) | -5.68 | -35.72 | -40.80 | -44.91 | -45.82 | / | / | / |
| 2. ( 1551.37) | -43.12 | -5.6 | -36.3 | -42.0 | -46.6 | / | / | / |
| 3. ( 1553.20) | -42.2 | -40.7 | -5.40 | -36.6 | 43.2 | / | / | / |
| 4. (1555.10) | -46.9 | -42.9 | -41.0 | -5.3 | -40.3 | -43.27 | -47.49 | / |
| 5. ( 1556.86) | /* | / | -41.7 | -40.1 | -5.68 | -38.5 | -46.1 | / |
| 6. ( 1558.79) | / | / | -41.9 | -41.9 | -38.3 | -5.59 | -40.1 | -45 |
| 7. ( 1560.62) | / | / | -43.6 | -43.5 | -42.3 | -33.5 | -5.58 | -39.2 |
| 8. ( 1562.65) | / | / | / | / | / | -39.9 | -31.7 | -5.49 |

Note: " / " means the crosstalks are not deectable

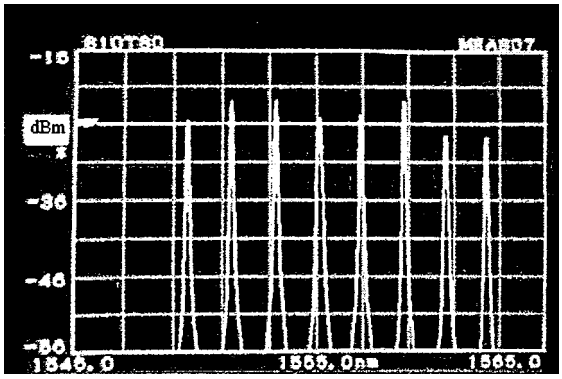


Fig. 3. Output spectrum from an eight channel V-grooved fiber array.

is good enough for optical communications network. The typical insertion loss of this system is in the neighborhood of $-5.5$ dB. Grating loss is a major factor of insertion losses. The diffraction efficiency of the holographic grating is 40% [9], which is due to the fixed index modulation and film thickness provided by DuPont photopolymers (DuPont Holographic Materials, Wilmington, DE) [13]. The measured optical 1 dB pass band is 0.2 nm which is corresponds 30 $\mu$m movement range of fiber array. The wide optical pass band makes the device robust to the variation of environmental temperature.

Fig. 3 shows the output spectrum from the eight-channel V-grooved fibers when input wavelength are 1549, 1551, 1553, 1555, 1557, 1559, 1561, and 1563 nm. The output spectrum is measured by a laser rather than a wide band white light source, so it shows the center wavelength of each individual channel rather than the exact loss spectrum of each channel because of the narrow line width and uneven input power of the laser. Epoxy injection and UV curing are used to fix all the optical components permanently. There is no observed component displacement after UV curing of epoxy.

## IV. SUMMARY

The designed DWDDM employs dispersion enhanced volume holographic grating and silicon V-grooved multimode fibers array with 250 $\mu$m spacing to demultiplex optical signal to eight-channel, namely at wavelength of 1549, 1551, 1553, 1555, 1557, 1559, 1561, and 1563 nm. The packaging losses of these channels are $-5.68$, $-5.6$, $-5.40$, $-5.3$, $-5.68$, $-5.59$, $-5.58$, and $-5.49$ dB, respectively. The typical cross-talk is $-35$ dB. All the components are permanently fixed with epoxy injection and UV cured, which makes the device robust and rigid.

## REFERENCES

[1] C. DeCusatis, "Optical data communication: Fundamentals and future directions," *Opt. Eng.*, vol. 37, no. 12, pp. 3082–3099, Dec. 1998.
[2] C. A. Brackett, "Dense wavelength division multiplexing networks: Principles and applications," *IEEE J. Select. Areas Commun.*, vol. 8, Aug. 1990.
[3] R. T. Chen and P. S. Guilfoyle, "Optoelectronic interconnects and packaging IV," *Proc. SPIE*, vol. 3005, pp. 144–154.
[4] M. K. Smit, "New focusing and dispersive planar component based on an optical phased array," *Electron. Lett.*, vol. 24, pp. 385–386, 1998.
[5] H. Takahashi, S. Suzuki, K. Kato, and I. Nishi, "Arrayed-waveguide grating for wavelength division multi/demultiplexer with nanometer resolution," *Electron. Lett.*, vol. 26, pp. 87–88, 1990.
[6] G. J. Cannell, A. Robertson, and R. Worthington, "Practical realization of a high density diodecoupled wavelength demultiplexer," *IEEE J. Select. Areas Commun.*, vol. 8, Aug. 1990.
[7] Y. Fujii, K.-I. Aoyama, and J.-I. Minowa, "Optical demultiplexer using a silicon Echelette grating," *IEEE J. Quantum Electron.*, vol. QE-16, pp. 165–169, Feb. 1980.
[8] F. N. Timofeev, P. Bayvel, J. E. Midwinter, and M. N. Sokolskii, "High-performance, free-space ruled concave grating demultiplexer," *Electron. Lett.*, vol. 31, pp. 1446–1467, Aug. 17, 1995.
[9] J. Liu and R. T. Chen, "Path-reversed photopolymer-based substrate-guided-wave optical interconnects for wavelength division demultiplexing," *Appl. Opt.*, vol. 38, no. 14, May 1999.
[10] L. A. Bergman, J. Morookian, and C. Yeh, "WDM component requirements for bit-parallel fiber optic computer networks," Tech. Rep., Dec. 1997.
[11] R. R. A. Syms, *Practical Volume Holography*. Oxford, U.K.: Clarendon, 1990.
[12] T. Niewulis, "Accessible fiber to the last mile," in *Proc. Symp. Opt. Internet 2000*, Dallas, TX, Jan. 18–20, 2000.
[13] W. Gambogi, K. Steijn, S. Mackara, T. Duzik, B. Hamzavy, and J. Kelly, "HOE imaging in DuPont holographic photopolymers," *Proc. SPIE*, vol. 2152, pp. 282–293, 1994.